UMT PRESS

Journal of Sustainability Science and Management
Journal Homepage: https://jssm.umt.edu.my
eISSN: 2672-7226
DOI: http://doi.org/10.46754/jssm.2026.06.006

ROLE OF CHITOSAN EXTRACT AS A CORROSION INHIBITOR IN ACIDIC ENVIRONMENT

MOHAMMAD FAKHRATUL RIDWAN ZULKIFLI[1], ADIB FARQIHIM[2], AHMED A AL-AMIERY[3,4], IZIONWORU VINCENT ONUEGBU[5], WAN MOHD NORSANI WAN NIK[1]*, ATRIA PRADITYANA[6], DINESH Y. DHANDE[7] AND JYOTI KAVIRAJWAR[8]

[1]*Faculty of Ocean Engineering Technology, Universiti Malaysia Terengganu, 21030 Kuala Nerus, Terengganu, Malaysia*
[2]*SPT Services Sdn. Bhd., Administration and Terminal Operation Building, Pengerang Integrated Complex (PIC), 81600 Pengerang, Johor, Malaysia*
[3]*Department of Chemical and Process Engineering, Faculty of Engineering and Built Environment, Universiti Kebangsaan Malaysia, 43400 Bangi, Selangor, Malaysia*
[4]*Biomedical Engineering Department, College of Engineering, Al-Ayen University (AUIQ), Nile St. Nasiriyah P.O. Box 64001, Dhi Qar, Iraq*
[5]*Department of Chemical/Petrochemical Engineering, Faculty of Engineering, Rivers State University, Nkpolu-Oroworukwo, Port Harcourt, Nigeria*
[6]*Department of Mechanical Industrial Engineering, Vocational Faculty, Institut Teknologi Sepuluh Nopember, Surabaya, 60111, Indonesia*
[7]*Department of Mechanical Engineering, AISSMS College of Engineering, Kennedy Road, Pune, 411001, India*
[8]*Department of School of Applied & Life Sciences, Uttaranchal University, Dehradun, Uttarakhand, 248007, India*

**Corresponding author: niksani@umt.edu.my*

ARTICLE INFO

Article History:
Received: 17 August 2025
Revised: 1 February 2026
Accepted: 3 February 2026
Published: 15 June 2026

Keywords:
Corrosion inhibitors, mild steel, chitosan, seawater

ABSTRACT

In marine industries, corrosion is a prevalent problem that poses threats to the durability, safety, and structural integrity of marine structures, equipment, and infrastructure. Traditional methods involved in corrosion control often rely on harmful and toxic inhibitors that would raise environmental and health concerns. Hence use of eco-friendly corrosion inhibitor is one of the best options to resolve this detrimental problem. In recent times, naturally available substances are gaining attention for effective corrosion inhibition. Chitosan, derived from chitin in shellfish exoskeletons is a biopolymer known for its biodegradability and non-toxicity. This study evaluated the efficiency of chitosan in inhibition of mild steel corrosion in seawater and acidic environments. Various parameters such as temperature, time, and concentration of inhibitor were assessed using Electrochemical Impedance Spectroscopy (EIS), gravimetric measurements, and Scanning Electron Microscopy (SEM) analysis. The results showed up to 89% inhibition efficiency at a temperature of 40°C, using 10 ml/L of chitosan, in accordance with the Langmuir adsorption isotherm, indicating physical adsorption with a free energy of ~ 20 kJ/mol.

Introduction

Corrosion is a significant and serious challenge faced by industries worldwide, posing severe threats not only to industrial systems but also to the natural environment. Its impact is far-reaching, causing extensive damage and leading to substantial economic losses, while also contributing to environmental degradation, material deterioration, structural breakdowns, and safety risks (Kiey *et al*., 2024). Implementation of corrosion inhibitors to avoid corrosion is a widely implemented technique (Zulkifli *et al*., 2021; Haque *et al*., 2023). Based upon the composition, there are two types of corrosion inhibitors - organic and inorganic. Further, they can be classified as anodic, cathodic, oxidising, non-oxidising, and adsorption inhibitors, based on their behaviour (Fernandes *et al*., 2019; Nabilah *et al*., 2022). Given their non-toxicity, affordability, and exceptional corrosion prevention capabilities, environmentally friendly organic corrosion inhibitors are being researched as potential substitutes for inorganic inhibitors.

Nitrate-based inhibitors, in particular, are emerging as a promising substitute due to their safe profile and compatibility with concrete, as they are commonly used as set accelerators (Gadioli *et al*., 2024). To achieve sustainable goals, corrosion inhibitors must be efficient, cost-effective, and environmentally degradable (Ilyos *et al*., 2023; Selma *et al*., 2023, 2025). According to the available literature, organic molecules play an effective role in corrosion and inhibition due to the existence of heteroatoms, non-bonded electrons, and π-bonded electrons (Shehnazdeep & Pradhan, 2022). The molecular structure of various organic compounds, particularly those with two or more atoms of O_2 or N_2 or S and unsaturated bonds, play a crucial role in inhibition (Haque *et al*., 2023). These compounds tend to inhibit corrosion more effectively than those containing only nitrogen or sulphur. The specific arrangement of these heteroatoms and bonds in the molecular framework is thought to be responsible for their enhanced corrosion-resistant properties (Mathiyan *et al*., 2017; Ibrahim *et al*., 2020).

The second most common naturally occurring green polymer is chitosan, which is mostly found in the fungal cell wall and arthropod exoskeleton. From a chemical perspective, it is an alkaline polysaccharide that is distinguished by the abundance of functional groups like amino group, glycosidic linkages in addition to primary and secondary hydroxyl groups (Obayes *et al*., 2017). Chitosan is a copolymer made of two different types of glucosamine: β-(1-4)-2-amido-2-deoxy-D-glucan, and N-acetylglucosamine, or β-(1-4)-2-acetamido-2-deoxy-D-glucan. It is extracted from chitin via partial deacetylation in alkaline medium (Elnaggar *et al*., 2024).

It is an excellent compound that can be alternately used when compared with conventional chemicals for preventing material corrosion, which includes antibacterial activity, biodegradability, and exceptional film-forming abilities (Zhang *et al*., 2020). Since chitosan has -NH groups and electronegative oxygen atoms, it can provide the active sites required for mild steel surfaces to interact chemically. Its potency as a corrosion inhibitor is increased by this quality (Li *et al*., 2013). To some extent, the inhibitory rate of chitosan has been enhanced by these chemical changes, but still, there is room to improve its inhibitory effectiveness even further, particularly at lower dosages (Ali *et al*., 2023). Additionally, not much research has been done on the inhibitory mechanisms of biodegradable polymers. Water-soluble and environmentally benign chitosan-based corrosion inhibitors are therefore advantageous to develop, especially for usage in maritime environments.

The applications for chitosan include the food, pharmaceutical, biomedical, textile, and agricultural sectors. It only dissolves in acidic solutions, such as diluted acetic acid, which limits its practical application in most solvents. Due to this drawback, a lot of studies have been done on chemically altering chitosan to enhance its mechanical, thermal, and solubility qualities, increasing its adaptability to a variety of conditions (Liu *et al*., 2024). Chemically, chitosan is made up of sugar glucosamine units that are repeated. Due to its structure, it is reactive and amenable to a variety of chemical changes. Chitosan's solubility and bioactivity can be improved by changing its chemical composition. For example, in research by John *et al*. (2024), chitosan is chemically modified to create a water-soluble derivative by reacting it with chloroacetic acid and vanillin. This modification enhances its utility in various applications, including corrosion inhibition and biomedical uses (John *et al*., 2024). People sometimes misinterpret chitosan and chitin as one and the same because of their close relationship.

Nevertheless, there are some ways in which chitosan varies from one another (Elieh-Ali-Komi & Hamblin, 2016). Chitosan is derived from a substance named chitin by deacetylation process, where some or all of the acetyl groups ($COCH_3$) are removed, converting N-acetylglucosamine units into glucosamine units (2-amino-2-deoxy-D-glucose). In chitosan, the amine group ($-NH_2$) is free, as the acetyl group has been removed. Chitosan shares β-(1→4) glycosidic linkages among its sugar units, much like chitin does. Chitin is made up of repeating N-acetylglucosamine units. Each repeating unit has an acetyl group ($COCH_3$) attached to the N atom in the amine group present on second carbon atom of glucose molecule. Chitin is linear polysaccharide possessing a stiff, crystalline structure.

Figure 1 depicts the key differences between chitosan and chitin and their chemical composition. The repeating unit in chitin is N-acetylglucosamine (GlcNAc), whereas in chitosan, the repeating unit is mainly glucosamine (GlcN), where the acetyl group is removed, leaving a free $-NH_2$ group at the 2^{nd} carbon (Elieh-Ali-Komi & Hamblin, 2016).

In the context of chitin and chitosan, acetylation is the process of forming N-acetylglucosamine units by attaching an acetyl group to the amine group ($-NH_2$) of glucosamine units (Hefni, 2024). Chitin has a high degree of acetylation, meaning that most of its amine groups are acetylated. In contrast, chitosan has a lower degree of acetylation, as the deacetylation process removes some or most of the acetyl groups, increasing the proportion of free amine groups (Ilyos *et al*., 2023). Solubility of chitin is less when compared with chitosan because it has more acetylation. The acetyl groups make it more hydrophobic, reducing its ability to interact with water molecules. Basically, chitin is insoluble in water due to its hydrophobic nature and crystalline structure. However, when chitin is immersed in strong acids like HCl, it breaks down the crystalline structure and protonates the acetylated amine groups, thus increasing its solubility. Since free amine groups exist and interact with water, particularly in acidic environments, chitosan is more soluble in this medium. The amine groups can protonate, meaning that they can gain a positive charge that can enhance their interaction with water (Kamaruzzaman *et al*., 2022).

In acidic medium, protonation of the amino groups occurs, hence the polymer Chitosan becomes more soluble, which in turn is due to increased interactions with water molecules and the formation of a polycationic polymer (Akakuru *et al*., 2018). The reactivity of both the polymers, i.e., chitin and chitosan are correlated to their chemical structure and functional groups present on the polymeric chains. Chitin has relatively lower reactivity compared to chitosan. The acetamido groups in chitin are relatively inert under mild conditions, which limits the reactivity of chitin. Its crystalline structure

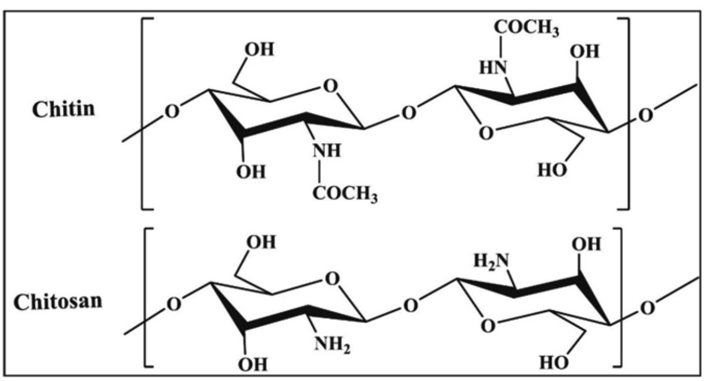

Figure 1: Structure of chitin and chitosan
Source: Hefni (2024)

also makes it less accessible to reagents, thus reducing its reactivity. In contrast, chitosan has much higher reactivity when compared to chitin. The presence of free amino groups makes chitosan much more reactive than chitin. These amino groups can participate in varied chemical reactions, like protonation, acylation and alkylation, cross-linking, Schiff Base formation, and quaternisation (Gao *et al*., 2023; Wan *et al*., 2025). In conclusion, although having the same basic structure and place of origin, chitin and chitosan differ greatly in their physical and chemical characteristics, especially reactivity and solubility, which has a big impact on how each is used in different industries.

This research specifically utilises and studies the usage and performance of chitosan as organic inhibitor. Literature reveals that the molecules containing amino and hydroxyl groups can easily interact with metal surfaces to create a shielding coating, acting as an obstruction, for corrosion-causing substances like water, chlorides, etc., on the metal surfaces (Kamaruzzaman *et al*., 2022). Through hydrogen bonding, chelation with metal ions, and electrostatic attraction, chitosan attaches to metal surfaces. The amino groups in chitosan can protonate and form bonds with metals in acidic medium enhancing the adhesion capacity of metals and provide protection. Chitosan molecules physically adsorb before congealing into a dense, sticky coating. By decreasing the rate of corrosion, this layer prevents corrosive species from spreading widely across the metal surface (Varun *et al*., 2024).

The main objective of this research is to investigate and synthesise an inhibitor that is both highly protective and ecologically benign by examining the effectiveness of chitosan's inhibition. The evaluation of inhibition efficiency from various concentrations of chitosan extract was done on mild steel, submerged in acidic media, which is 1 M HCl and also artificial seawater with different temperatures to mimic the harsh conditions of the marine environment (Jiyaul *et al*., 2023). The structure of the chitosan composite was investigated using Fourier Transform Infrared Spectroscopy (FTIR) technique. EIS technique was utilised to study the inhibition efficiency.

Materials and Methods

Preparation of Mild Steel Plates for Corrosion Study

The steel sheet was cut into small plates of (2 cm x 2 cm). They were polished with sandpapers with various grit sizes (220, 600, 2,000, and 5,000). Distilled water was used for cleaning and then degreasing was done using ethanol. Each coupon has a hole punched through its centre that allow threads to be knotted for suspension in a medium. Vacuum oven at 60°C was used for drying the steel coupons (Ikhmal *et al*., 2017).

Preparation of HCl Solution

To create an acid electrolyte, analytical grade HCl was utilised. It was diluted with double-distilled water, and to ensure that there is no contamination, a new 1 M HCl solution was used for every experiment (Al-Amiery *et al*., 2023).

Preparation of Chitosan Powder

High-purity chitosan powder was used for the research work. Materials and apparatus that are needed to dissolve the chitosan powder includes 1% acetic solution, distilled water, and a magnetic stirrer with a heating plate. A chitosan solution was prepared using 0.5 g of chitosan powder and 100 ml of 1% solution of acetic acid.

A magnetic stirrer was used to mix the solution. This process was continued until chitosan was fully dissolved, then agitated for two to four hours at room temperature or slightly higher (30°C to 50°C) and then it was filtered to remove any undissolved particles.

Weight Loss Method

After being cleaned as per ASTM specifications, mild steel plates were weighed using a Shimadzu sensitive electronic scale. Subsequently, they were immersed in 1 M hydrochloric acid solution in the presence and absence of chitosan for 90 minutes. Then coupons were boiled in a mixture of zinc dust and sodium hydroxide to remove any last traces of corrosion products. Ultimately, the coupons underwent a distilled water rinse, drying process, and reweighting (Nik *et al*., 2010).

Electrochemical Measurement (PDP and EIS)

Three electrode system was used to study potentiodynamic polarisation (PDP) and electrochemical impedance spectroscopy (EIS). Mild steel plate acted as the working electrode (WE), saturated calomel electrode (SCE) as a reference electrode, and platinum electrode as the auxiliary electrode (AE). SCE is positioned close to the steel electrode as feasible for each measurement. Zsimp Win software was utilised for all electrochemical measurements. All three electrodes were dipped in a 1 M HCl solution for one hour before each measurement, in order to maintain a constant OCP (open circuit potential). Electrochemical analysis was carried out using a stable open circuit voltage. The amplitude of the AC pulses employed in the testing was 10 mV, and their frequency range of 0.1 Hz to 10 kHz. Tafel tests on mild steel were carried out using an open circuit potential with a sweep rate of 1 mV/s and potentials ranging from +250 mV to -250 mV. Corrosion potential (E_{corr}) and current density of corrosion (I_{corr}) were measured via potentiodynamic polarisation; in this case, the I_{corr} is given by the extrapolated intercept of the anodic and cathodic Tafel plots. The study of kinetics of the electrochemical reaction occurring at WE was done by Tafel analysis. These observations can be used to create a corrosion inhibition strategy that works (John *et al*., 2024).

Scanning Electron Microscopic Studies

SEM (Model AIS2300C) was utilised to analyse the morphological structure of mild steel in the presence and absence of chitosan solution. Before the study, the steel plates were immersed in 1 M hydrochloric acid solution at 30°C for 3 hours (Hassan *et al*., 2016).

Results and Discussions

Weight Loss Method (Gravimetric Measurement)

The rate at which corrosion deepens over time is known as the rate of corrosion (*CR*), and it is often expressed as milligrams per cm^2 per hour (mg/cm^2/h). It was calculated with this formula:

$$CR = \frac{\text{weight loss (mg)}}{\text{area (cm}^2) \times time\ (hours)} \quad (1)$$

The percentage of inhibition efficiency (*IE*%) was calculated using the formula given below, where CR_0 denotes corrosion rate in the absence of inhibitor, while CR_i denotes the corrosion rate with various concentrations of the chitosan extract inhibitor.

$$\%IE = \frac{CR_0 - CR_i}{CR_0} \times 100 \quad (2)$$

The rate of corrosion and efficiency of inhibition were measured under varying parameters, such as temperature and inhibitor concentration, for 24 test coupons. Results obtained are shown in Table 1.

The weight loss data, in terms of corrosion rate, for metal steel submerged in acidic medium with varying concentrations of inhibitor (chitosan extract) is shown in Figure 2. It can be calculated that the highest recorded corrosion rate is equivalent to 25.9 mg/cm^2/h.

After 90 minutes of immersion, inhibited mild steel plate experienced 8.5 mm per year corrosion rate. For plates in which chitosan extract was included in the solution, the corrosion rate dropped to 7.8, 7.1, 6.4, 5.7, and 5.1 mmpy. Further increase in the inhibitor concentration showed only a slight improvement, indicating that the inhibitor's effectiveness had nearly plateaued. This shows that even a small amount of chitosan extract inhibitor can significantly decrease the corrosion rate of mild steel plates.

Table 1: Calculated values of corrosion inhibition efficiency in the absence and presence of different concentrations of inhibitor and temperatures

Coupon No.	Temperature (K)	Inhibitor Concentration (ml/L)	Inhibitor Efficiency (*IE%*)
1	301	0	0
2	301	2	73.0
3	301	4	75.4
4	301	6	83.0
5	301	8	84.0
6	301	10	87.8
7	313	0	0
8	313	2	72.7
9	313	4	80.0
10	313	6	84.5
11	313	8	88.1
12	313	10	89.0
13	323	0	0
14	323	2	58.3
15	323	4	77.0
16	323	6	79.5
17	323	8	81.5
18	323	10	87.5
19	333	0	0
20	333	2	47.9
21	333	4	69.4
22	333	6	75.0
23	333	8	77.7
24	333	10	86.1

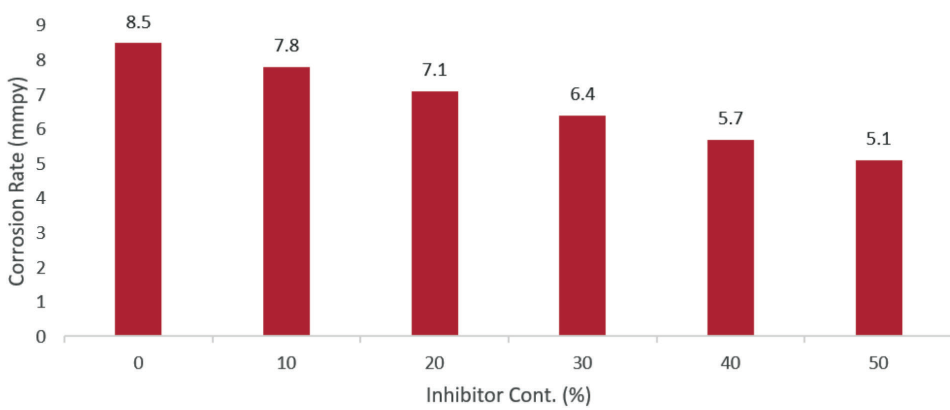

Figure 2: Corrosion rate of mild steel at room temperature immersed for 90 minutes in varying concentration of chitosan extract

Electrochemical Impedance Spectroscopy (EIS)

Figure 3 depicts the Nyquist impedance plot which clearly indicates that adding the chitosan extract inhibitor at any concentration completely changes the impedance response of steel plates. Two key aspects can be interpreted from the plot. The first is the radius of the semicircle- larger radii indicate higher concentrations. The second is the diameter of the capacitive loop, which also increases with the concentration of the chitosan extract inhibitor, meaning the diameter of the capacitive loops corresponds to the semicircle radius.

The efficiency of the inhibitor was determined using Equation (3):

$$IE\% = \left(\frac{R_{ct} - R_{cto}}{R_{ct}}\right) \times 100 \quad (3)$$

where R_{ct^o} and R_{ct} represent the charge transfer resistance in the absence and presence of chitosan extract, respectively.

Table 2 depicts inhibitor efficiency (*IE*%) and impedance parameters obtained from the Nyquist plots. As previously noted, R_{ct} (polarisation resistance) value increases and (double-layer capacitance) value decreases as the concentration of chitosan extract inhibitor increases, which may be due to adsorption of chitosan extract on mild steel surface. It indicates that the capacitance values fall with increasing chitosan extract inhibitor concentrations, polarisation resistance values increase.

Double-layer capacitance, or is given as:

$$C_{dl} = Y_o\,(\omega_{max})^{\,n-1} \quad (4)$$

where Y_o is the Constant Phase Element (CPE) constant and is the angular frequency at which the imaginary part of impedance is maximised (rad/s). It can be calculated by using the formula , where *f* is the frequency. Last is , which is the parameter deviation for the CPE: -1 ≤ ≤ 1. Figure 4 shows the equivalent circuit that was used to fit in EIS data; data were depicted graphically by Nyquist plots shown in Figure 3.

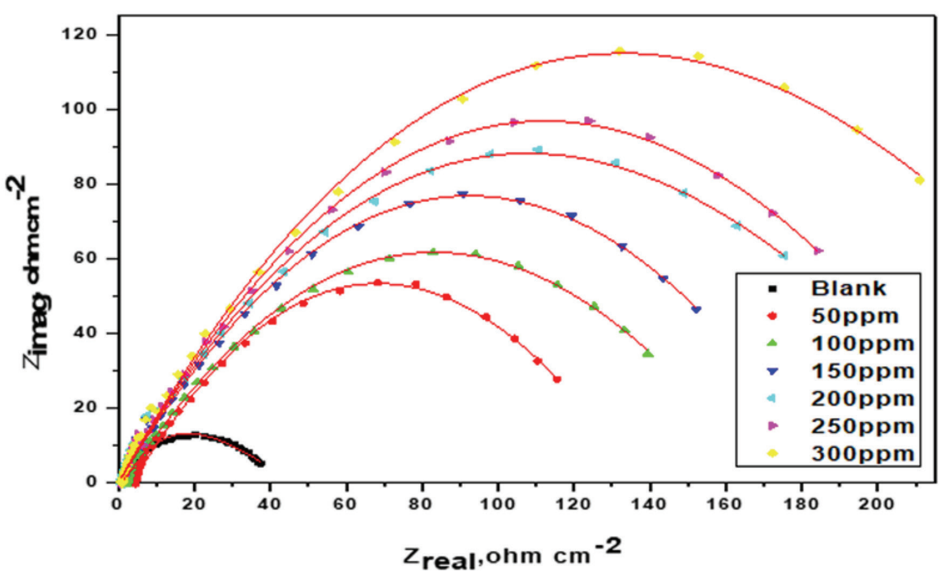

Figure 3: Nyquist plots for mild steel in 1 M HCl in the presence and absence of varying concentrations of chitosan extract

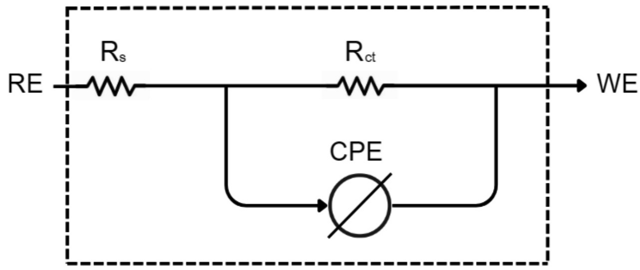

Figure 4: Electrochemical circuit

Thermodynamic Corrosion Parameters

Figure 5 shows the Arrhenius plot for the corrosion rate of mild steel (k_{corr}) after two hours of immersion in 1 M HCl, both in presence and absence of the chitosan extract. From these plots, the activation energy (E_a) can be determined using the formula:

$$Log\ (k_{corr}) = \log(A) - \frac{E_a}{2.303RT} \quad (5)$$

where:

kcorr = Corrosion rate
A = Frequency factor (pre-exponential factor)
E_a = Activation energy
R = Universal gas constant
T = Absolute temperature

To calculate the change in enthalpy, *ΔH* and change in entropy, *ΔS* of activation for the corrosion reaction, the transition state theory equation is used, which is displayed in Figure 6. This method involves plotting $\left(\frac{k_{corr}}{T}\right)$ against $\left(\frac{1}{T}\right)$ and using the slope to intercept the resulting line:

$$Log\ \left(\frac{k_{corr}}{T}\right) = \left(log\left(\frac{R}{Nh}\right) + \frac{\Delta S}{2.303R}\right) - \frac{\Delta H}{2.303RT} \quad (6)$$

where:

kcorr = The corrosion rate
T = Absolute temperature (K)
N = Avogadro's number
h = Planck's constant
ΔS = Activation entropy
ΔH = Activation enthalpy

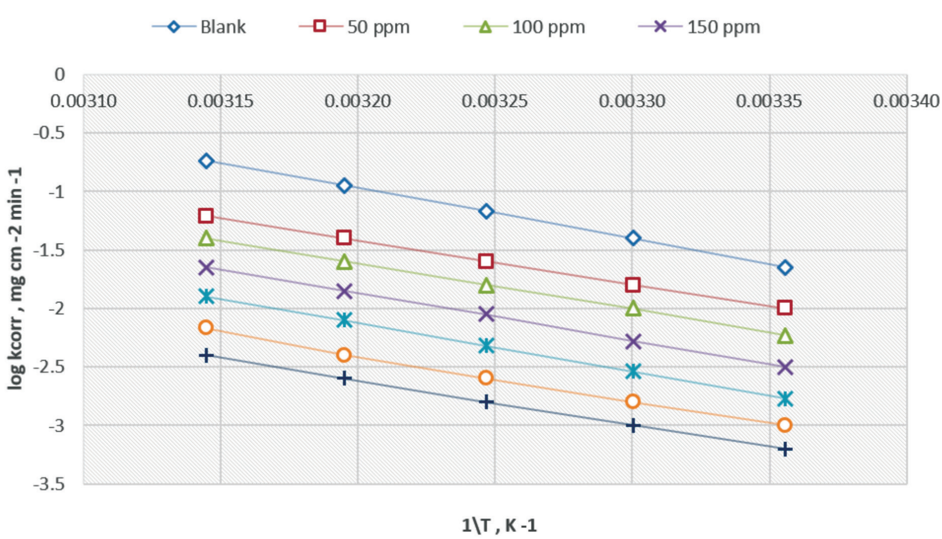

Figure 5: Arrhenius plot for corrosion of mild steel (k_{corr}) after two hours of immersion in 1 M HCl

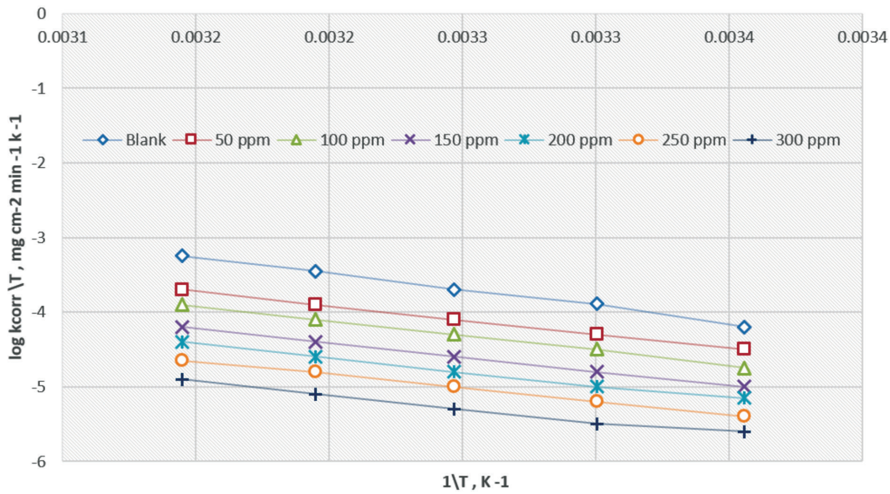

Figure 6: Transition-state log plots of $\left(\frac{k_{corr}}{T}\right)$ vs. $\left(\frac{1}{T}\right)$ for corrosion of mild steel after two hours of immersion time in 1 M hydrochloric acid in the absence and presence of chitosan extract at various concentrations

The results in Figures 5 and 6 show that the thermodynamic activation energy barrier has been enhanced and the corrosion inhibition was achieved by physical adsorption mechanism. Kiey *et al*. (2024) achieved similar results.

Adsorption Isotherms

This study discusses three types of isotherms: Langmuir, Temkin, and Freundlich isotherms. To prove that the chitosan extract follows Langmuir adsorption isotherms, demonstration in Figure 7 was made. The following formula was used in the calculation:

$$\frac{C}{\theta} = \frac{1}{K_{ads}} + C \qquad (7)$$

where:

θ = Surface coverage
K_{ads} = Adsorption equilibrium constant
C = Concentration of inhibitor

Figure 7 shows that the performance of chitosan additive can be explained using the Langmuir adsorption isotherm. Literature revealed similar results (Zhang *et al*., 2020). By plotting θ against C, it yields straight line with slope 1 and an intercept of K_{ads}. Figure 8 displays the plots of standard Gibbs free energy of adsorption, ΔG^{o}_{ads} and it can be determined using the following formula:

$$K_{ads} = (1/1000)^{(-\Delta G^{\circ}{ads/RT})} \qquad (8)$$

where:

K_{ads} = Adsorption equilibrium constant
ΔG^{o}_{ads} = Standard Gibbs free energy of adsorption
R = Universal gas constant (8.314 J/mol·K)
T = Absolute temperature (K)
1000 = Concentration of water in ml/L

For Freundlich isotherms, which is plotted in Figure 9, it can be calculated using this formula:

$$\theta = K_{ads} \cdot C^{n} \qquad (9)$$

where:

C = Concentration of inhibitor
K_{ads} = Adsorption equilibrium constant
θ = Surface coverage
n = Intensity of adsorption

The Temkin isotherm model explains adsorption by accounting the contact between the adsorbent (surface) and adsorbate (adsorbed molecules). This model is based on two key ideas: first idea states that as more molecules get adsorbed on the surface, the heat of adsorption gradually decreases in straight-line (linear) manner. This happens because the adsorbed molecules interact with each other and also with the surface. The second idea states that the surface has uniform binding sites, which means the energy with which molecules attach to the surface is evenly distributed up to a certain maximum binding energy. Unlike the Freundlich isotherm, which assumes that the decrease in adsorption energy follows a logarithmic trend, the Temkin isotherm assumes a linear decrease in heat of adsorption as surface coverage increases (Liu *et al.*, 2024).

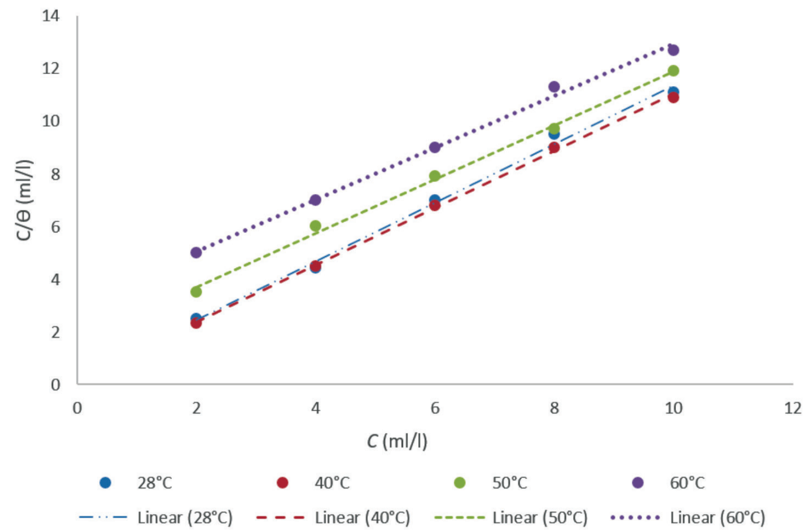

Figure 7: Langmuir adsorption isotherm of mild steel in 1 M HCl at various conditions

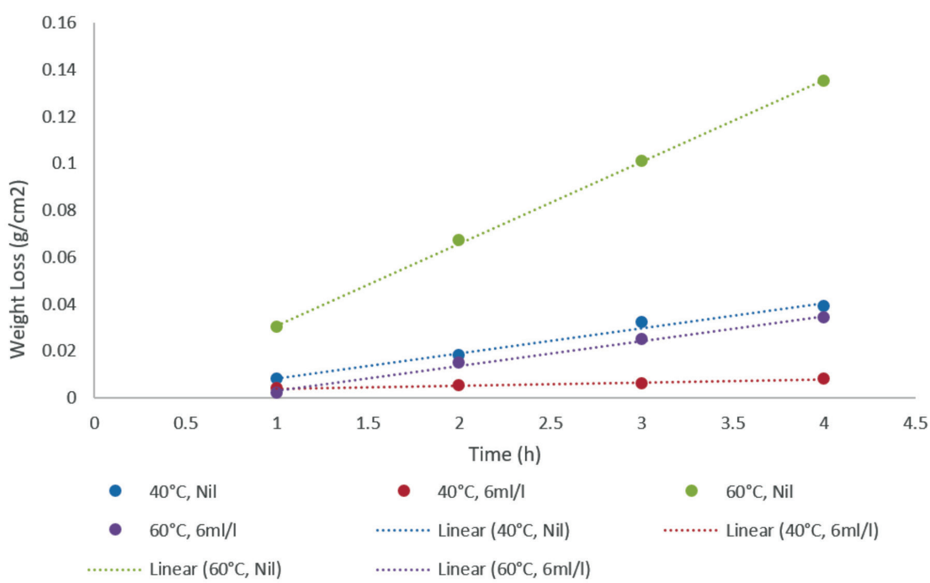

Figure 8: Zero order reaction kinetics of mild steel in 1 M HCl

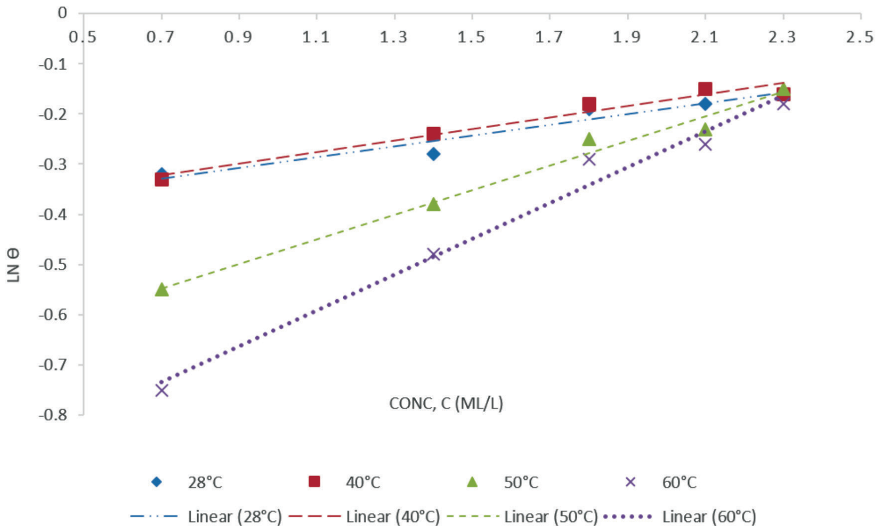

Figure 9: Freundlich adsorption isotherm of mild steel in 1 M HCl at various conditions

Potentiodynamic Polarisation (PDP)

The efficacy and the corrosion inhibition were evaluated by potentiodynamic polarisation (PDP). It entails measuring the current density that results from continuously sweeping the voltage of the working electrode. Surface redox processes happen to mild steel when it is submerged in corrosive fluids. Tafel graph with and without the chitosan extract inhibitor were prepared to demonstrate the disintegration of mild steel. Tafel plots help in explaining the mild steel corrosion mechanism.

Referring to Table 3 data, it can be concluded that the Tafel slopes (βa and βc) show that the inhibitor acts as a mixed-type inhibitor. The parallel Tafel lines show that the corrosion mechanism remains unchanged in the presence of the inhibitor. Inhibitor efficiency percentage (*IE%*) increases as the concentration of the chitosan extract rises, whereas the corrosion current density (i_{corr}) decreases, as shown in Table 3. This suggests that the extract reduces the corrosion of mild steel in 1 M HCl. β_a and β_c values change slightly with an increase in inhibitor extract concentration, clearly indicating that the extract affects both metal dissolution and hydrogen evolution (Pradityana *et al.*, 2024).

Table 3: Data from PDP of mild steel immersed in 1 M HCl at multiple concentrations

Conc. (ppm)	i_{corr} **(µA cm^{-2})**	**-E_{corr} (mV vs SCE)**	**βc mV dec^{-1}**	**βa mV dec^{-1}**	k_{corr} **mpy**	*θ*	***IE%***
0	156	549	228.2	71.9	345.42	-	-
50	149	547	169.2	79.7	68.03	0.803	80.3
100	146	543	124.9	86.4	67.04	0.806	80.6
150	140	541	117.4	54.6	66.92	0.815	81.5
200	123	536	172.5	87.0	64.01	0.837	83.7
250	102	533	103.4	77.3	56.41	0.865	86.5

Fourier Transform Infrared (FTIR) Spectroscopy

FTIR was used to recognise the structure of molecule. Figure 10 shows the FTIR spectrum of mild steel that was immersed in a solution containing chitosan extracts. From the FTIR spectrum shown on Figure 10, there are three functional groups that can be identified, which are hydroxyl group, carbonyl group, and carbon-carbon double bond.

These three functional groups imply that the chitosan extract's phenolic chemicals are important for preventing corrosion. These functional groups probably produce a protective layer that helps stop corrosion by adhering to the mild steel surface.

Scanning Electron Microscopy (SEM)

Figures 11 and 12 show the micrographs of mild steel corroded in different environments, both in the presence and absence of an inhibitor. SEM studies infer that in the presence of an inhibitor, very mild corrosion is observed, but it becomes severe in the absence of an inhibitor.

Figure 11 illustrates heavy corrosion of the mild steel in 1 M HCl. In contrast, Figure 12 shows that surface condition improves with the presence of the inhibitor in 1 M HCl, depending on the concentration of the inhibitor solution. These studies help to understand that the chitosan extract inhibitor protects the metal surface by forming an adsorbed layer.

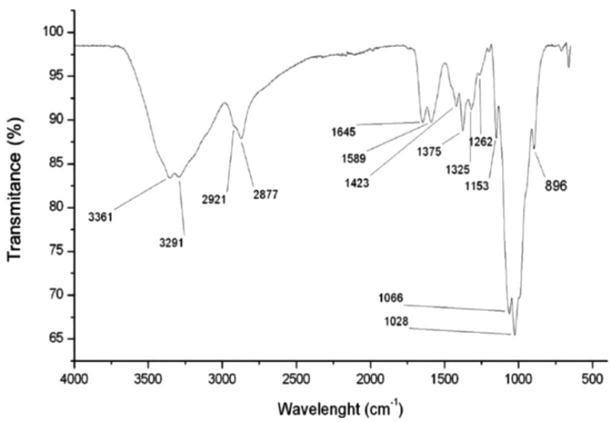

Figure 10: FTIR spectrum of mild steel exposed to corrosion inhibited 1 M HCl

(a) Hydroxyl/amine group: 3361 cm^{-1} and 3291 cm^{-1}
(b) Polysaccharides (C=H): 1375 cm^{-1}
(c) *β*- (1 → 4) glycosidic linkage: 896 cm^{-1}

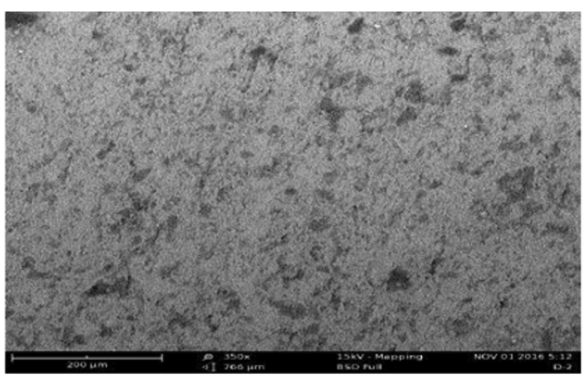

Figure 11: Micrograph of corroded mild steel immersed in 1 M HCl in the absence of inhibitor

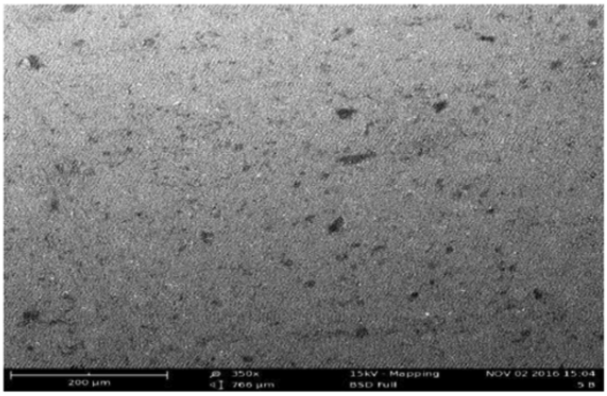

Figure 12: Micrograph of corroded mild steel immersed in 1 M HCl in the presence of inhibitor

Conclusions

The study investigated the efficiency of chitosan, a natural biopolymer, as an efficient corrosion inhibitor for steel in marine environments. The results demonstrate that chitosan significantly reduces corrosion, particularly in acidic conditions. The corrosion inhibition increases with increase in concentration of chitosan, reaching up to 89% at optimal conditions. The study also reveals that chitosan's performance is influenced by factors such as temperature and concentration, with higher temperatures slightly reducing its effectiveness. Furthermore, the study validates that chitosan adsorption on the steel surface, follows the Langmuir isotherm model, suggesting physical adsorption. Considering all parameters, chitosan can be assumed as a good alternative for the conventional harmful corrosion inhibitors, in terms of both effectiveness and environmental friendliness, which makes it a viable option for preventing corrosion in industrial and marine structures.

Acknowledgements

This research was supported by UMT-UKM-RSU Matching Grant Corrosion project (UMT/MG1+2/2025/ 53594). We also would like to acknowledge the Ministry of Higher Education Malaysia (FRGS/1/2021/STG05/UMT/01/1-Corrosion Inhibition).

Conflict of Interest Statement

The authors agree that this research was conducted in the absence of any self-benefits, commercial, or financial conflicts and declare the absence of conflicting interests with the funders.

References

Akakuru, O. U., Louis, H., Amos, P. I., Akakuru, O. C., Nosike, E. I., & Ogulewe, E. F. (2018). The chemistry of chitin and chitosan justifying their nanomedical utilities. *Biochemistry & Pharmacology*, *7*(1), 241. https://doi.org/10.4172/2167-0501.1000241

Al-Amiery, A. A., Betti, N., Isahak, W. N., Al-Azzawi, W. K., & Nik, W. M. (2023). Exploring the effectiveness of Isatin–Schiff base as an environmentally friendly corrosion inhibitor for mild steel in hydrochloric acid. *Lubricants*, *11*(5), 211. https://doi.org/10.3390/lubricants11050211

Ali, M. I., Khudair, N. A., Huseeni, M. D., Kadhim, M. M., & Khadom, A. A. (2023). Electrochemical polymerization of new Schiff base monomer as an anti-corrosion coating on carbon steel in saline water: Experimental and theoretical studies. *Journal of Bio- and Tribo-Corrosion*, *9*, 40. https://doi.org/10.1007/s40735-023-00758-5

Elieh-Ali-Komi, D., & Hamblin, M. R. (2016). Chitin and chitosan: Production and application of versatile biomedical nanomaterials. *International Journal of Advanced Research*, *4*(3), 411–427. https://www.ncbi.nlm.nih.gov/pmc/articles/PMC5094803/

Elnaggar, E. M., Abusaif, M. S., Abdel-Baky, Y. M., Ragab, A., Omer, A. M., Ibrahim, I., & Ammar, Y. A. (2024). Insight into divergent chemical modifications of chitosan biopolymer: Review. *International Journal of Biological Macromolecules*, *277*, 134347. https://doi.org/10.1016/j.ijbiomac.2024.134347

Fernandes, C. M., Fagundes, T. S., Santos, N. E., Rocha, T. S., Garrett, R., Borges, R. M., Muricy, G., Valverde, A. L., & Ponzio, E. A. (2019). *Ircinia strobilina* crude extract as corrosion inhibitor for mild steel in acid medium. *Electrochimica Acta*, *312*, 137–148. https://doi.org/10.1016/j.electacta.2019.04.148

Gadioli, A. O., Menezes, L., Pereira, E. C., Monteiro, S. N., & Azevedo, A. R. G. (2024). Imidazolium-based ionic liquids as corrosion inhibitors for stainless steel in different corrosive media: An overview. *Journal of Materials Research and Technology*, *29*, 803–823. https://doi.org/10.1016/j.jmrt.2024.01.066

Gao, K., Qin, Y., Liu, S., Wang, L., Xing, R., Yu, H., Chen, X., & Li, P. (2023). A review of the preparation, derivatization and functions of glucosamine and *N*-acetyl-glucosamine from chitin. *Carbohydrate Polymer Technologies and Applications*, *5*, 100296. https://doi.org/10.1016/j.carpta.2023.100296

Haque, J., Saleh, T. A., Murmu, M., Chauhan, D. S., Wan Nik, W. B., Banerjee, P., & Quraishi, M. A. (2023). Synthesis of multi donating sites grafted on graphene oxide nanosheets: Anti-corrosion study for mild steel in 1 M HCl with DFT calculations. *Journal of Molecular Liquids*, *389*, 122820. https://doi.org/10.1016/j.molliq.2023.122820

Haque, J., Zulaikha, M. A., Wan, W. B., Daoudi, W., Berdimurodov, E., & Zulkifli, F. (2023). *Alocasia odora* extract as environmentally benign corrosion inhibitor for aluminum in HCl. *Moroccan Journal of Chemistry*, *11*(4), 1013–1026. https://doi.org/10.48317/IMIST.PRSM/morjchem-v11i04.41618

Hassan, K. H., Khadom, A. A., & Kurshed, N. H. (2016). *Citrus aurantium* leaves extracts as a sustainable corrosion inhibitor of mild steel in sulfuric acid. *South African Journal of Chemical Engineering*, *22*, 1–5. https://doi.org/10.1016/j.sajce.2016.07.002

Hefni, H. H. H. (2024). Functional chitosan surfactants for corrosion inhibition in petroleum industry. *International Journal of Biological Macromolecules*, *278*, 134704. https://doi.org/10.1016/j.ijbiomac.2024.134704

Ibrahim, N. F., Abdullah, W. R. W., Rooshde, M. S., Ghazali, M. S. M., & Nik, W. B. W. (2020). Corrosion inhibition properties of epoxy-zinc oxide nanocomposite coating on stainless steel 316L. *Solid State Phenomena*, *307*, 285–290. https://doi.org/10.4028/www.scientific.net/SSP.307.285

Ikhmal, W. M. K., Yasmin, M. Y. N., Fazira, M. F. M., Rafizah, W. A., Wan, W. B., & Sabri, M. G. M. (2017). Anticorrosion coating using *Olea* sp. leaves extract. *IOP Conference Series: Materials Science and Engineering*, *344*, 012028. https://doi.org/10.1088/1757-899X/344/1/012028

Ilyos, E., Elyor, B., Khusan, Y., Javokhir, A., Omar, D., Avni, B., Wan, W. B., Abduvali, K., & Khamdam, A. (2023). Supramolecular corrosion protection: Eco-friendly synthesis and efficacy of a β-cyclodextrin/*o*-phenylenediamine complex. *Journal of the Taiwan Institute of Chemical Engineers*, *147*(6), 104944. https://doi.org/10.1016/j.jtice.2023.104944

Jiyaul, H., Mohammad, F. R. Z., Nabilah, I., Mumtaz, A. Q., Mohd, S. M. G., Elyor, B., & Wan, W. N. (2023). Environmentally benign water-soluble sodium L2-(1-Imidazolyl) alkanoic acids as new corrosion inhibitors for mild steel in artificial seawater. *ACS Omega*, *8*, 24797–24812. https://doi.org/10.1021/acsomega.3c00366

John, S., Zachariah, P. M., Augustine, C., James, B. G., Joseph, B., & Sarath, J. M. K. (2024). Corrosion inhibition of mild steel in 1 M HCl using water soluble chitosan derivative of vanillin. *International Journal of Biological Macromolecules*, *262*, 130024. https://doi.org/10.1016/j.ijbiomac.2024.130024

Kiey, A., Mohamed-Ezzat, R. A., & Sawsan, D. (2024). Eco-friendly anti-corrosion performance of chitosan modified with fused heterocyclic compound on mild steel in acidic medium. *International Journal of Biological Macromolecules*, *263*, 130133. https://doi.org/10.1016/j.ijbiomac.2024.130133

Li, M., Xu, J., Li, R., Wang, D., Li, T., Yuan, M., & Wang, J. (2013). Simple preparation of aminothiourea-modified chitosan as corrosion inhibitor and heavy metal ion adsorbent. *Journal of Colloid and Interface Science*, *417*, 131–136. https://doi.org/10.1016/j.jcis.2013.11.053

Liu, S., Zhou, J., Liang, G., Lyu, X., & Li, Z. (2024). Evaluation of green corrosion inhibitors of chitosan oligosaccharide derivatives for CO2 corrosion inhibition on 20# carbon steel. *Process Safety and Environmental Protection*, *190*. https://doi.org/10.1016/j.psep.2024.07.052

Mathiyan, M., Ramdas, S., Surendran, S., Nattamai, S., Bhuvanesh, P., & Anandaram, S. (2017). *N*(1)-pentyl isatin-*N*(4)-methyl-*N*(4)-phenyl thiosemicarbazone (PITSc) as a corrosion inhibitor on mild steel in HCl. *Journal of Alloys and Compounds*, *695*, 171–182. https://doi.org/10.1016/j.jallcom.2016.10.173

Nabilah, I., Siti, M. M., Mohammad, F. R. Z., Vincent, O. I., Mariyam, J. G., & Nik, W. N. (2022). A review on application of marine algae as green corrosion inhibitors in acid medium. *Vietnam Journal of Chemistry*, *60*(4), 409–416. https://doi.org/10.1002/vjch.202200001

Nik, W. B. W., Sulaiman, O., Giap, S. G. E., & Rosliza, R. (2010). Evaluation of inhibitive action of sodium benzoate on corrosion behaviour of AA6063 in seawater. *International Journal of Technology*, *1*(1), 20–28. https://doi.org/10.14716/ijtech.v1i1.39

Obayes, H. R., Al-Amiery, A. A., Alwan, G. H., Thamer, A. A., Amir, A., & Abu, B. M. (2017). Sulphonamides as corrosion inhibitor: Experimental and DFT studies. *Journal of Molecular Structure*, *1138*, 27–34. https://doi.org/10.1016/j.molstruc.2017.02.100

Pradityana, A., Khosfirah, F., Biwai, F. N., Shidieqqy, R. H., Hakim, M. L., Santosa, P. I., & Wan Nik, W. B. (2024). Curry leaf extract (*Murraya koenigii* (L.) Spreng) as a corrosion inhibitor of ASTM A36 steel in H2SO4 solution. *Results in Engineering*, *24*, 103037. https://doi.org/10.1016/j.rineng.2024.103037

Selma, L., Walid, D., Abdelmalik, E. A., Omar, D., Avni, B., Asma, B., Wan, W. B., Abdelkader, Z., & Abdellatif, L. (2023). Comparative study of the performance and inhibitory efficiency of two new organic heterocyclic in the chemical industry. *Materials Science and Engineering: B*, *297*, 116779. https://doi.org/10.1016/j.mseb.2023.116779

Selma, L., Walid, D., Omar, D., Ibrahim, A. N., Wan, M. N. W. N., Avni, B., Hansang, K., Abdelmalik, E. A., Abdelkader, Z., & Abdellatif, L. (2025). Promising corrosion resistance of mild steel, copper, and aluminum in hydrochloric acid solution using an environmentally friendly corrosion inhibitor. *Journal of Industrial and Engineering Chemistry*, *146*, 332–348. https://doi.org/10.1016/j.jiec.2024.11.016

Shehnazdeep, N., & Pradhan, B. (2022). A study on effectiveness of inorganic and organic corrosion inhibitors on rebar corrosion in concrete: A review. *Materials Today: Proceedings*, *65*, 1360–1366. https://doi.org/10.1016/j.matpr.2022.04.296

Varun, P., De, S., & Dutta, J. (2024). Synthesis and characterization of citric acid-modified chitosan Schiff base with enhanced antibacterial properties for the elimination of Bismarck Brown R and Rhodamine B dyes from wastewater. *International Journal of Biological Macromolecules*, *264*, 130664. https://doi.org/10.1016/j.ijbiomac.2024.130664

Wan, M. N. W. N., Jiyaul, H., Mohd, S. M. G., Atria, P., Izionworu, V. O., Walid, D., Elyor, B., & Ahmed, A. A. (2025). Amino acid-derived imidazole zwitterion as green interfacial corrosion inhibitor for cold rolled steel. *Case Studies in Chemical and Environmental Engineering*, *11*, 101103. https://doi.org/10.1016/j.cscee.2025.101103

Zhang, Q. H., Hou, B. S., Li, Y. Y., Zhu, G. Y., Liu, H. F., & Zhang, G. A. (2020). Two novel chitosan derivatives as high efficient eco-friendly inhibitors for the corrosion of mild steel in acidic solution. *Corrosion Science*, *164*, 108346. https://doi.org/10.1016/j.corsci.2019.108346

Zulkifli, M. F. R., Shamsul, B. S. N., Abdullah, S., Mohd, G. M. S., & Wan, W. M. N. (2021). *Citrus aurantifolia* leaf extract as a potential anti-corrosion additive in alkyd paint for mild steel. *Journal of Sustainability Science and Management*, *16*(3), 10–20. https://doi.org/10.46754/Jssm.2021.04.002